Supplementary materials
An fMRI-based brain marker predicts individual differences in delay discounting

Leonie Koban[1,2,*]
Sangil Lee[3]
Daniela S. Schelski[4,5]
Marie-Christine Simon[6]
Caryn Lerman[7]
Bernd Weber[4,5]
Joseph W. Kable[3]
Hilke Plassmann[1,2]

[1] Marketing Area, INSEAD, Fontainebleau, France
[2] Control-Interoception-Control Team, Paris Brain Institute (ICM), INSERM U 1127, CNRS UMR 7225, Sorbonne University, Paris, France
[3] Department of Psychology, University of Pennsylvania, Philadelphia, PA, USA
[4] Center for Economics and Neuroscience, University of Bonn, Bonn, Germany
[5] Institute of Experimental Epileptology and Cognition Research, University of Bonn, Germany
[6] Institute for Nutrition Science, University of Bonn, Bonn, Germany
[7] Norris Comprehensive Cancer Center, University of Southern California Los Angeles, CA, USA

* Email: leonie.koban@icm-institute.org

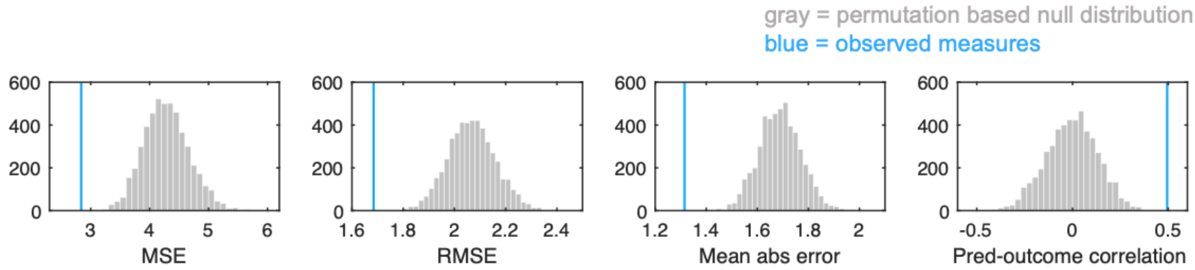

Fig. S1. Results of the permutation test (Study 1). Log(k) values were randomly permuted, and the prediction algorithm was repeated on the permuted brain-outcome data 5000 times in order to generate null distributions for standard accuracy metrics (from left to right): mean squared error (MSE), root mean squared error (RMSE), mean absolute error (mean abs error), and prediction-outcome correlation (for additional interpretability). Histograms of null distribution are shown in gray bars, observed metrics in blue. For all metrics, observed values were outside the range of permutation samples (all p's < 0.002).

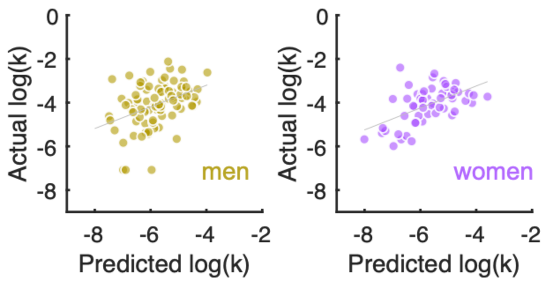

Fig. S2. Correlations between predicted and observed log(k) were significant in both male and female participants (Study 2).

Suppl. Table S3. Significant positive and negative weights contributing to the *k*-marker during CHOICE (FDR corrected $q < 0.05$ across the whole feature space, i.e. three concatenated gray-matter-masked whole brain maps, and at least three contingent voxels). In the column "Atlas label", cortical regions (Ctx) are labeled based on the multimodal cortical parcellation by Glasser et al. [1], basal ganglia regions are based on Pauli et al. [2], cerebellar regions on Diedrichsen, et al. [3], and brainstem regions based on a combination of studies [4,5]. The entire combined anatomical atlas is available on Github: https://github.com/canlab/Neuroimaging_Pattern_Masks/tree/master/Atlases_and_parcellations/2018_Wager_combined_atlas. This repository includes multiple atlases and other meta-analytic and multivariate maps. Tools for manipulating and analyzing this and other atlases are in the CANlab Core Tools repository: https://github.com/canlab/CanlabCore.

Positive weights

Name	Atlas label	Volume (voxels)	MNI Coordinates X	Y	Z	max(z)
Orbitofrontal cortex	Ctx_a47r_L	29	-34	40	-12	4.49
Anterior insula	Ctx_FOP5_R	114	32	24	4	4.45
Midtemporal gyrus	Ctx_PHT_R	18	68	-48	4	4.43
Frontal pole/vmpFC	Ctx_10pp_L	29	-8	60	-12	4.42
Midtemporal gyrus	Ctx_TE1a_R	6	66	-4	-24	4.24
Temporal operculum	Ctx_LBelt_L	32	-42	-28	2	4.21
Other	No_label	9	-2	-28	14	4.13
Visual cortex	Ctx_V2_R	18	20	-100	0	4.04
Orbitofrontal cortex	Ctx_a47r_L	11	-44	38	-12	4.03
Ventrolateral prefrontal cortex	Ctx_45_L	72	-50	28	-2	4.03
Striatum	V_Striatum_R	38	18	26	0	3.99
Striatum	V_Striatum_L	22	0	4	-2	3.96
Orbitofrontal cortex	Ctx_11l_L	13	-18	42	-14	3.95
Retrosplenial cortex	Ctx_RSC_R	15	2	-46	8	3.94
Temporal operculum	Ctx_PoI1_L	20	-38	-4	-16	3.89
Visual cortex	Ctx_V4_R	3	30	-92	22	3.86
Other	No_label	3	66	-54	8	3.84
Visual cortex	Ctx_V3_L	3	-22	-94	24	3.82
Midtemporal gyrus	Ctx_TE1a_L	14	-64	-10	-14	3.79
Amygdala	Ctx_PeEc_R	5	20	6	-26	3.75
Caudate	Cau_L	3	-26	-32	20	3.72
Precentral gyrus	Ctx_4_L	9	-12	-26	70	3.71
Temporal pole/amygdala	Ctx_TGd_R	7	34	12	-24	3.65
Visual cortex	Ctx_V2_L	4	-14	-102	14	3.62
Midtemporal gyrus	Ctx_TGd_R	4	52	4	-26	3.59
Orbitofrontal cortex	Ctx_13l_L	4	-28	28	-14	3.48

Negative weights

Name	Atlas label	Volume (voxels)	X	Y	Z	max(z)
Midcingulate cortex	Ctx_24dv_R	58	8	0	36	-5.03
Cerebellum	Cblm_CrusII_L	130	-24	-76	-40	-4.87
Superior frontal gyrus	Ctx_SFL_L	106	-8	10	70	-4.83

Visual cortex	Ctx_ProS_R	79	24	-52	4	-4.81
Inferior parietal lobule	Ctx_PF_L	338	-54	-30	42	-4.75
Precuneus	Ctx_7Am_L	67	-2	-56	60	-4.63
Posterior cingulate cortex	Ctx_23c_R	51	8	-24	40	-4.35
Parietal cortex	Ctx_PGs_R	17	38	-70	52	-4.28
Parahippocampal cortex	Ctx_VMV2_L	7	-32	-50	-6	-4.06
Midcingulate cortex	Ctx_p24pr_L	20	-6	2	36	-4.00
Parahippocampal cortex	Ctx_ProS_L	13	-20	-48	-2	-3.99
Intraparietal sulcus	Ctx_7PC_L	11	-44	-42	60	-3.94
Cerebellum	Cblm_CrusI_R	6	50	-48	-28	-3.88
vmPFC	Ctx_9m_L	8	-8	50	16	-3.87
Cerebellum	Cblm_CrusI_L	6	-46	-64	-42	-3.87
Midcingulate cortex	Ctx_33pr_L	6	-2	22	20	-3.84
Inferior parietal lobule	Ctx_PF_R	13	54	-34	46	-3.83
Inferior frontal cortex	Ctx_6r_L	3	-54	4	16	-3.80
Dorsolateral prefrontal cortex	Ctx_9_46d_R	4	20	48	26	-3.68

Suppl. Table S4. Significant positive and negative weights contributing to the k-marker for the parametric modulation by LL AMOUNT (FDR corrected $q < 0.05$ across the whole feature space, i.e. three concatenated gray-matter-masked whole brain maps, at least three contingent voxels).

Positive weights

Name	Atlas label	Volume (voxels)	MNI Coordinates X	Y	Z	max(z)
Medial frontal gyrus	Ctx_8BM_R	386	-2	26	36	5.86
Dorsolateral prefrontal cortex	Ctx_6a_R	199	26	8	52	5.80
Intraparietal Sulcus	Ctx_PFm_R	288	48	-36	52	5.72
Orbitofrontal cortex	Ctx_11l_R	50	16	30	-24	5.55
Inferior parietal lobule	Ctx_PGs_R	298	38	-74	36	5.40
Dorsolateral prefrontal cortex	Ctx_SCEF_L	131	-14	14	52	5.12
Precuneus	Ctx_POS2_R	177	12	-66	38	5.12
Cingulate cortex	Ctx_d32_R	114	10	34	22	4.93
Inferior frontal cortex	Ctx_IFJa_L	134	-44	8	26	4.88
Ventromedial prefrontal cortex	Ctx_p32_L	24	-12	44	4	4.80
Cerebellum	Cblm_IX_R	18	4	-50	-34	4.75
Orbitofrontal cortex	Ctx_11l_L	37	-24	44	-18	4.66
Dorsolateral prefrontal cortex	Ctx_p9_46v_L	67	-46	28	22	4.66
Visual cortex	Ctx_V1_R	29	18	-76	12	4.66
Intraparietal Sulcus	Ctx_AIP_L	24	-38	-44	42	4.61
Inferior parietal lobule	Ctx_IP1_L	58	-32	-72	32	4.57
Posterior cingulate cortex	Ctx_23d_R	56	-2	-28	36	4.56
Anterior insula	Ctx_AVI_L	58	-32	20	2	4.55
Ventrolateral prefrontal cortex	Ctx_a9_46v_R	66	42	46	10	4.47
Ventrolateral prefrontal cortex	Ctx_a9_46v_L	35	-36	44	6	4.40
Ventromedial prefrontal cortex	Ctx_p32_R	47	8	42	0	4.27
Anterior insula	Ctx_AVI_R	16	32	20	2	4.19
Posterior cingulate cortex	Ctx_RSC_R	7	6	-16	32	4.06
Ventromedial prefrontal cortex	Ctx_10r_L	13	-12	38	-8	4.05
Parahippocampal cortex	Ctx_PeEc_R	5	26	-22	-30	4.04
Cerebellum	Cblm_VI_R	11	34	-50	-28	4.02
Thalamus/Pulvinar	Thal_Pulv	10	-12	-32	0	4.00
Medial temporal cortex	Ctx_PreS_R	11	14	-36	0	3.99
Cerebellum	Cblm_CrusI_R	10	40	-40	-38	3.99
Orbitofrontal cortex	Ctx_OFC_L	3	-8	50	-24	3.98
Dorsolateral prefrontal cortex	Ctx_p9_46v_R	9	46	34	24	3.72
Precuneus	Ctx_POS2_R	8	14	-60	24	3.70
Ventrolateral thalamus	Thal_VL	7	-12	-12	14	3.65
Cerebellum	Cblm_VI_L	6	-34	-56	-26	3.61
Precuneus	Ctx_POS2_L	3	-12	-68	36	3.55

Negative weights

Name	Atlas label	Volume (voxels)	X	Y	Z	max(z)
Visual cortex	Ctx_V2_L	142	-8	-80	-10	-5.51
Visual cortex	Ctx_V4t_L	70	-42	-82	0	-4.99
Cerebellum	Cblm_CrusI_L	148	-28	-80	-30	-4.93
Cerebellum	Cblm_CrusI_R	64	24	-84	-30	-4.85
Superior frontal cortex	Ctx_SFL_R	47	4	6	68	-4.85
Paracentral lobule	Ctx_4_R	37	6	-30	60	-4.83
Superior parietal lobule	Ctx_7AL_L	158	-20	-40	64	-4.63
Parahippocampal cortex	Ctx_VMV1_R	59	20	-44	-10	-4.60
Visual cortex	Ctx_V3A_L	94	-12	-86	24	-4.51
Superior temporal sulcus	Ctx_STSdp_L	78	-50	-32	-6	-4.49
Cerebellum	Cblm_V_L	16	-22	-34	-30	-4.49
Midcingulate cortex	Ctx_24dv_L	21	-8	-2	40	-4.40
Parahippocampal cortex	Ctx_VMV1_L	32	-18	-60	-8	-4.36
Superior frontal cortex	Ctx_8BL_R	35	2	50	46	-4.28
Visual cortex	Ctx_V4t_R	48	44	-78	-2	-4.23
Visual cortex	Ctx_V3_R	41	16	-72	-8	-4.22
Superior frontal cortex	Ctx_8BL_R	15	4	30	62	-4.20
Superior parietal lobule	Ctx_7AL_R	14	18	-44	70	-4.13
Putamen	Putamen_Pp_R	3	28	-12	10	-4.10
Putamen	Putamen_Pp_L	10	-30	-22	10	-4.06
Superior frontal cortex	Ctx_9a_L	24	-10	62	26	-4.05
Paracentral lobule	Ctx_SCEF_L	11	-8	-6	66	-4.05
Visual cortex	Ctx_V3A_R	31	20	-90	18	-4.00
Frontal pole	Ctx_10d_R	7	12	68	16	-3.90
Temporal pole	Ctx_PeEc_L	4	-28	-4	-34	-3.87
Visual cortex	Ctx_MT_R	9	48	-68	4	-3.83
Superior temporal gyrus	Ctx_PSL_L	17	-56	-36	16	-3.80
Precuneus	Ctx_5L_R	6	12	-48	66	-3.80
Visual cortex	Ctx_V4_R	8	32	-78	-10	-3.79
Superior temporal gyrus	Ctx_A4_L	4	-60	-30	10	-3.70
Temporal pole	Ctx_TE1a_L	4	-52	-6	-32	-3.70
Superior temporal sulcus	Ctx_STV_R	6	50	-42	10	-3.68
Superior temporal gyrus	Ctx_PSL_R	5	54	-32	22	-3.56

Suppl. Table S5. Significant positive and negative weights contributing to the k-marker for the parametric modulation by DELAY (FDR corrected q < 0.05 across the whole feature space, i.e. three concatenated gray-matter-masked whole brain maps, at least three contingent voxels).

Positive weights

Name	Atlas label	Volume (voxels)	MNI Coordinates X	Y	Z	max(z)
Visual cortex	Ctx_V3A_R	131	12	-86	20	5.30
Ventromedial prefrontal cortex	Ctx_10v_R	160	2	42	-20	5.14
Precuneus	Ctx_PCV_L	102	-10	-54	46	4.75
Superior temporal sulcus	Ctx_STSdp_L	63	-54	-34	4	4.71
Superior temporal gyrus	Ctx_TA2_R	59	52	-8	-2	4.66
Precentral gyrus	Ctx_3b_L	214	-34	-26	62	4.62
Angular gyrus	Ctx_PGi_R	27	40	-60	22	4.61
Ventromedial prefrontal cortex	Ctx_9m_R	37	16	48	6	4.58
Putamen	Putamen_Pp_L	35	-32	-14	2	4.43
Caudate	Cau_L	36	-22	22	2	4.35
Superior temporal gyrus	Ctx_TPOJ1_R	29	50	-30	8	4.34
Angular gyrus	Ctx_PGi_L	43	-48	-54	22	4.34
Precentral gyrus	Ctx_4_L	5	-32	-16	44	4.33
Cingulate sulcus	Ctx_24dd_L	49	-6	-10	48	4.29
Subgenual cingulate cortex	Ctx_s32_L	17	-10	26	-12	4.24
Paracentral lobule	Ctx_5L_R	28	10	-40	62	4.16
Midcingulate cortex	Ctx_24dv_R	9	10	-4	44	4.15
Cerebellum	Cblm_CrusII_L	3	-12	-84	-44	4.04
Caudate	Cau_R	7	6	26	-4	3.99
Superior frontal gyrus	Ctx_9m_R	21	4	56	38	3.97
Midtemporal gyrus	Ctx_MT_R	9	46	-68	12	3.96
Visual cortex	Ctx_V1_L	14	-14	-82	-4	3.94
Cerebellum	Cblm_CrusII_R	7	28	-84	-44	3.93
Posterior insula/temporal operculum	Ctx_52_R	16	40	-22	-2	3.91
Superior temporal sulcus	Ctx_A5_L	8	-58	2	-10	3.90
Paracentral lobule	Ctx_5mv_R	4	18	-32	44	3.83
Cerebellum	Cblm_CrusI_R	10	40	-74	-34	3.82
Midtemporal gyrus	Ctx_A5_L	4	-62	-12	-10	3.80
Superior parietal lobule	No_label	4	-22	-44	50	3.78
Paracentral lobule	Ctx_5m_L	11	-10	-44	64	3.77
Paracentral lobule	Ctx_5mv_R	7	16	-24	44	3.72
Inferior frontal cortex	Ctx_45_L	5	-54	26	14	3.72
Precentral gyrus	Ctx_6d_L	3	-26	-18	62	3.72
Superior parietal lobule	Ctx_7Am_L	5	-4	-66	62	3.70
Visual cortex	Ctx_V2_L	8	-6	-86	18	3.69
Visual cortex	Ctx_IP0_R	6	30	-70	22	3.68
Caudate	Cau_L	4	-18	8	18	3.68

Posterior cingulate cortex	Ctx_24dd_R	7	10	-20	44	3.66
Superior parietal lobule	Ctx_2_L	3	-18	-38	60	3.63
Superior temporal sulcus	Ctx_STV_R	3	58	-34	8	3.57

Negative weights

Name	**Atlas label**	**Volume (voxels)**	**X**	**Y**	**Z**	**max(z)**
Dorsolateral prefrontal cortex	Ctx_a9_46v_L	76	-40	50	14	-5.20
Brainstem	Bstem_Ponscd	54	2	-28	-36	-4.78
Intraparietal sulcus	Ctx_7PC_L	34	-40	-46	48	-4.70
Dorsolateral prefrontal cortex	Ctx_8C_R	26	40	12	30	-4.57
Brainstem	Bstem_Ponscd_L	69	-12	-38	-36	-4.54
Paracentral lobule	Ctx_4_R	12	6	-30	78	-4.41
Inferior parietal lobule	Ctx_PFm_R	23	54	-44	52	-4.39
Cerebellum	Cblm_Dentate_R	39	18	-42	-36	-4.25
Cerebellum	Cblm_IX_L	51	-6	-54	-36	-4.23
Medial frontal gyrus	Ctx_8BM_R	45	0	22	42	-4.17
Orbitofrontal cortex	Ctx_a10p_R	5	22	58	-10	-4.16
Visual cortex	Ctx_V4_R	19	30	-86	-10	-4.11
Paracentral lobule	Ctx_SFL_R	10	4	-2	76	-4.10
Thalamus	Thal_Pulv	13	-4	-30	4	-4.08
Orbitofrontal cortex	Ctx_11l_R	17	22	32	-18	-4.07
Visual cortex	Ctx_LO2_L	3	-46	-82	-6	-4.07
Anterior insula/frontal operculum	Ctx_AVI_R	3	36	26	-4	-4.06
Dorsolateral prefrontal cortex	Ctx_p9_46v_R	52	44	36	16	-3.99
Cerebellum	Cblm_CrusII_R	3	8	-86	-28	-3.92
Frontal pole	Ctx_a10p_R	9	28	66	-6	-3.85
Thalamus	Thal_Pulv	19	6	-26	8	-3.85
Orbitofrontal cortex	Ctx_pOFC_R	8	16	10	-16	-3.84
Midcingulate cortex	Ctx_a32pr_L	4	-8	34	24	-3.84
Visual cortex	Ctx_V4_L	10	-34	-90	-6	-3.80
Frontal pole	Ctx_a10p_L	3	-20	60	-10	-3.80
Visual cortex	Ctx_V3CD_L	9	-44	-86	12	-3.79
Superior parietal lobule	No_label	3	28	-38	76	-3.79
Posterior cingulate cortex	Ctx_31a_L	9	0	-32	44	-3.74
Inferior parietal lobule	Ctx_PFm_L	4	-50	-48	52	-3.69
Frontal pole	Ctx_p10p_L	3	-30	66	0	-3.65
Visual cortex	Ctx_VVC_R	4	30	-62	-14	-3.63
Nucleus Accumbens	NAC_L	6	-10	4	-18	-3.57
Nucleus Accumbens	NAC_L	3	-8	12	-10	-3.52

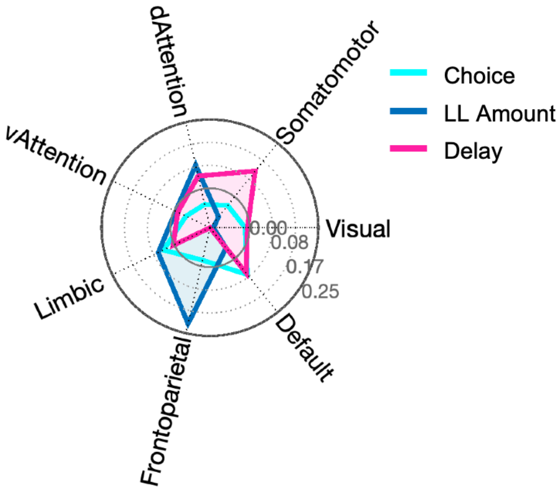

Fig. S6. **Spatial similarity of the *k-marker* with seven established large-scale functional resting-state networks [6].** The spatial correlation (Pearson's *r*) of the *k*-marker patterns with each network [6] with each component map of the *k*-marker (Choice, LL Amount, Delay) is displayed in a radar plot. The *k*-marker pattern for the Choice contrast did not correlate strongly with any given resting state network (highest of r = 0.074 with the Default network). The pattern for the LL-Amount contrast correlated positively with the Frontoparietal network (FPN) (r = 0.22), indicating that higher activity in this network—often associated with cognitive control—for greater LL amounts predicts *greater* delay discounting. Negative correlations were seen with the Visual and Somatosensory networks, in line with the findings reported above. In contrast, the pattern for the Delay contrast correlated positively with the Somatomotor network (r = 0.12) and negatively with the FPN (r = -0.15). This suggests that networks may contribute with different signs to different aspects of decision-making. While increased FPN activity for increasing LL amounts predicts greater discounting, increased FPN activity for increasing delays predicts *lower* discounting. Paralleling the meta-analytical similarity results in the main text, this suggests that the relationship between control-related activity and discounting is less clear-cut than previously thought.

Supplementary References

1 Glasser, M. F. *et al.* A multi-modal parcellation of human cerebral cortex. *Nature* **536**, 171-178, doi:10.1038/nature18933 (2016).

2 Pauli, W. M., O'Reilly, R. C., Yarkoni, T. & Wager, T. D. Regional specialization within the human striatum for diverse psychological functions. *Proc. Natl. Acad. Sci. U. S. A.* **113**, 1907-1912, doi:10.1073/pnas.1507610113 (2016).

3 Diedrichsen, J., Balsters, J. H., Flavell, J., Cussans, E. & Ramnani, N. A probabilistic MR atlas of the human cerebellum. *Neuroimage* **46**, 39-46, doi:10.1016/j.neuroimage.2009.01.045 (2009).

4 Bär, K.-J. *et al.* Functional connectivity and network analysis of midbrain and brainstem nuclei. *Neuroimage* **134**, 53-63, doi:10.1016/j.neuroimage.2016.03.071 (2016).

5 Shen, X., Tokoglu, F., Papademetris, X. & Constable, R. T. Groupwise whole-brain parcellation from resting-state fMRI data for network node identification. *Neuroimage* **82**, 403-415, doi:10.1016/j.neuroimage.2013.05.081 (2013).

6 Yeo, B. T. T. *et al.* The organization of the human cerebral cortex estimated by intrinsic functional connectivity. *J. Neurophysiol.* **106**, 1125-1165, doi:10.1152/jn.00338.2011 (2011).